Geotech Geol Eng (2011) 29:597–610
DOI 10.1007/s10706-011-9406-0

ORIGINAL PAPER

Discrete-Element Computation of Averaged Tensorial Fields in Sand Piles Consisting of Polygonal Particles

Pradip Roul · Alexander Schinner · Klaus Kassner

Received: 21 August 2010 / Accepted: 25 April 2011 / Published online: 7 May 2011

Abstract This work is a contribution to the understanding of the mechanical properties of non-cohesive granular materials in the presence of friction and a continuation of our previous work (Roul et al. 2010) on numerical investigation of the macroscopic mechanical properties of sand piles. Besides previous numerical results obtained for sand piles that were poured from a localized source ("point source"), we here consider sand piles that were built by adopting a "line source" or "raining procedure". Simulations were carried out in two-dimensional systems with soft convex polygonal particles, using the discrete element method (DEM). First, we focus on computing the macroscopic continuum quantities of the resulting symmetric sand piles. We then show how the construction history of the sand piles affects their mechanical properties including strain, fabric, volume fraction, and stress distributions; we also show how the latter are affected by the shape of the particles. Finally, stress tensors are studied for asymmetric sand piles, where the particles are dropped from either a point source or a line source. We find that the behaviour of stress distribution at the bottom of an asymmetric sand pile is qualitatively the same as that obtained from an analytical solution by Didwania and co-workers (Proc R Soc Lond A 456:2569–2588, 2000).

Keywords Discrete element method (DEM) · Sand pile · Representative volume element (RVE) · Stress · Strain · Fabric

P. Roul (✉)
Institute of Mathematics, Potsdam University,
14469 Potsdam, Germany
e-mail: drpkroul@yahoo.com

P. Roul · K. Kassner
Institute of Theoretical Physics, Otto-Von-Guericke
University Magdeburg, Postfach 4120,
39106 Magdeburg, Germany

A. Schinner
T-Systems, Dachauer Straße 665,
80995 München, Germany

1 Introduction

During the last few years, extensive research has been devoted to the study of the mechanical properties of granular materials. To some extent, this is due to their importance in applications within various industrial branches such as the pharmaceutical, agricultural, geotechnical, and energy production industries. On the other hand, granular media are also interesting from a fundamental point of view—so far no generally applicable coherent theoretical description for their macro-states is available, a situation that calls for more scientific activity.

In particular, the stress distribution under a sand pile has attracted much attention, based on theoretical (Bouchaud et al. 1995; Wittmer et al. 1996, 1997; Cantelaube and Goddard 1997; Didwania et al. 2000; Tejchman and Wu 2008; Claudin et al.

1998), experimental (Jotaki and Moriyama 1979; Smid and Novosad 1981; Zhao et al. 2003; Vanel et al. 1999; Brockbank et al. 1997; Zuriguel et al. 2007; Zuriguel and Mullin 2008) and numerical studies (Luding 1997; Matuttis 1998; Matuttis et al. 2000; Liffman et al. 2001; Li et al. 2005). The pressure under a sand pile may exhibit quite counterintuitive features. In some cases, there is a local minimum (dip) in the pressure profile below the tip of the pile whereas in others, there is not (Vanel et al. 1999). Moreover, the pressure distribution is affected by the shape of the particles. If a sand pile contains a mixture of elongated particles poured from a point source, the pressure distribution displays a deep minimum beneath the apex of the pile. On the other hand, if it contains a mixture of particles with an aspect ratio close to 1—we will call these *equiaxed* particles—then there rather is a small minimum (Zuriguel et al. 2007; Zuriguel and Mullin 2008).

The phenomenon of the ''*dip under the heap*'' has fascinated physicists. On the other hand, among engineers there was a tendency to discard it as an isolated phenomenon without particular significance, for which many different explanations may be found, and which is probably due to different reasons in different experimental situations. One trivial explanation was that the plate onto which the sand was poured bent downward during the process (Zhao et al. 2003), which would immediately reduce the pressure at the centre, providing only that the sand did not follow this movement without resistance. While this explanation may hold for some experiments, there have been careful studies in the meantime with thick ground plates in Refs. (Vanel et al. 1999; Brockbank et al. 1997; Zuriguel et al. 2007; Zuriguel and Mullin 2008) for which such an effect can essentially be excluded and which still lead to a pressure minimum. Moreover, in simulations a deflection of the bottom of the system is excluded by definition, nevertheless they reproduce the pressure minimum (Luding 1997; Matuttis 1998; Matuttis et al. 2000; Liffman et al. 2001; Li et al. 2005).

Apart from the stress distribution discussed above, another major mechanical property of granular material is its density distribution, which may be calculated from the local volume fraction of the granular aggregate and the density of its constituent particles. It is clearly important to understand how density is distributed inside materials for application in chemical industry, science, soil mechanics, and concrete production. The bulk density of granular aggregates also displays interesting properties. In some cases, it exhibits a relatively homogeneous distribution inside the heap, in others, it is very inhomogeneous. The result depends strongly on the characteristics of the granulate, especially the shape and size distributions of the particles as discussed by Picard et al. (Picard et al. 2001). Moreover, with the same material, the construction history of the heap of materials plays a crucial role. If a heap is constructed from a rainy (uniform) filling method, producing what is called a layered sequence in (Matuttis 1998), there is a homogeneous density distribution in the heap, if it is constructed from a point source via a so-called wedge sequence (Matuttis 1998) then there is an inhomogeneous density distribution, such as the one observed experimentally by Smid and co-workers (Smid et al. 1993).

The structural properties of force chains in two-dimensional sand piles were measured experimentally by Zuriguel et al. (2007) and it was found that the shape of the particles has a major influence on the packing of granular materials leading to different force chain structures in the sand piles. They reported that the chain structures for piles consisting of circular particles are open whereas force chain patterns are more complex for piles consisting of elongated particles.

In order to investigate the influence of the construction history of sand piles and the shape distribution of particles on their mechanical properties, we simulate sand piles by either pouring grains from a point source or from a line source onto a flat substrate until a pile emerges. Our study is based on numerical experiments on sand piles by implementing a well-established numerical technique, the so-called *discrete element method (DEM),* proposed by Cundall et al. (Cundall and Strack 1979), which will help us to investigate the mechanical properties inside the piles.

This article is organized as follows. In Sect. 2, we first give a short description of the simulation method used in this work. We then describe how a sand pile is constructed using two different types of pouring procedures in Sect. 3. Section 4 is devoted to the definition of macroscopic fields including stress, strain and fabric tensors. The numerical results of microscopic force distributions and several averaged macroscopic variables obtained from our DEM

simulations for both types of sand piles are presented in Sect. 5. The influence of the construction history of a sand pile is examined for stress distributions under *asymmetric* sand piles and numerical results for stress distributions are qualitatively compared with available analytical predictions for the stress tensor in such a situation in Sect. 6. Finally, in Sect. 7, we summarize and discuss our main results.

2 Simulation Method

We use the discrete element method (DEM) for simulating sand piles in a two-dimensional system, i.e. essentially molecular dynamics with more complex particles and force laws including dissipation. The behaviour of an assembly of N grains can be obtained numerically by integrating Newton's and Euler's equations of motion Eq. (1), involving the forces and the torques acting on each particle. We use a fifth-order Gear predictor–corrector scheme (Gear 1971) with a fixed time step in order to solve the equation of motion for all particles. Particles are represented by convex polygons.

$$\begin{aligned} m_i\ddot{r}_i &= F_i + \sum_{j=1}^{N} F_{ij} \\ I_i\ddot{\phi}_i &= M_i + \sum_{j=1}^{N} M_{ij}. \end{aligned} \tag{1}$$

Here, m_i is the mass of the particle i. F_i is the force acting on particle i due to the gravitational field. F_{ij} is the contact force on particle i exerted by particle j ($F_{ii} = 0$, and $F_{ij} = 0$, if particle j does not touch particle i). Since the direction of the force will not point to the centre of mass of a particle in general, each force produces a torque M_{ij} about that centre (and of course, $M_{ii} = 0$). This will lead to an angular acceleration $\ddot{\phi}_i$; I_i is the moment of inertia of particle i about its centre of mass. So particle rotations are fully taken into account in our simulation. M_i stands for the external torque acting on the particle, which however vanishes here, $M_i = 0$, because gravity is the only external force, which does not induce torques about the centres of mass of the particles. Time is advanced after the initialization procedure of the assembly until the latter has relaxed to a steady state.

Since we consider non-cohesive particles in our simulation, the only interaction forces between two particles are friction forces and repulsion on contact. In DEM with soft particles, the particles may overlap which is exploited in the force calculation. The repulsive *normal* force is computed using the geometry of the overlap: it is taken proportional to the overlap area of the two colliding particles, its direction is perpendicular to the *contact line*, the straight line joining the two intersection points of the particle polygons. A distance mimicking elastic displacement is calculated from the overlap area and a characteristic length. The latter is proportional to the harmonic mean of the lengths of the two branch vectors pointing from the centres of mass of the particles to their common contact and it is almost constant during a collision. Its precise definition is given in (Roul et al. 2010; Schinner 2001). In order to have a realistic simulation, the overlap distance must be small in comparison with the particle size. To make collisions inelastic, a dissipative normal force is included in our algorithm. The calculation of the *tangential* force F_t, which is parallel to the contact line, is more complicated than that of the normal force F_n, because it is to be determined from the Coulomb condition $|F_t| \leq \mu F_n$, where μ is the static friction coefficient; this is just an inequality, not an evaluable formula. A detailed analytic description of both the normal and tangential force calculations may be found in (Roul et al. 2010; Schinner 2001).

The force calculation is one of the most time-consuming parts of the algorithm. Therefore, in order to reduce computing time, algorithms from virtual reality and computational geometry were adapted as explained in (Schinner 1999). In our simulation system, walls are represented as big immobile particles. An essential aspect to make the algorithm robust is the convexity of the polygons involved. If one uses non-convex polygons, the definition of the contact line may become ambiguous, because more than two intersection points may arise, and large overlaps can happen easily, because there is no simple algorithm for the calculation of the distance of non-convex polygons, and this can lead to local energy explosions. The basic reason for using polygonal particles instead of, say circular and elliptic ones is that polygons are believed to better approximate shapes of true grains that are often faceted. It has been shown (Hidalgo et al. 2009; Azéma and Radjai

2010) that for static assemblies the behaviour of faceted particles may be very different from that of "round" particles (having no flat surfaces).

3 Method of Preparation of the Sand Pile

One may construct a sand pile in many different ways. Here, we restrict ourselves to two different approaches (both of technological relevance). The first consists in pouring the material from a funnel with a small outlet, known as a "point source" and the second in pouring the material in a uniformly distributed way from a so-called "line source". Note that the line source is reduced in length during the procedure so as to have a length equal to or slightly smaller than that of the top plateau of the pile at any instant of time. When a pile is constructed from a point source (wedge sequence), the particles are dropped onto the apex of the sand pile and roll down the slopes of the pile, as shown in Fig. 1a. On the other hand, when a sand pile is constructed from a line source (layered sequence), the particles are dropped in a layer-wise manner, from a height that is slightly more than one particle diameter above the highest present layer, as shown in Fig. 1b, which means that they have little kinetic energy on impact.

3.1 Sand Piles from a Point Source

Sand piles were constructed from several thousands of soft convex polygonal particles using the wedge sequence. We used poly-disperse mixtures of particles with varying shapes, sizes and edge numbers for simulating a pile. The particles were dropped onto the system from 40 cm height with initial velocity of 0.2 m/s and a time interval of 0.1 s between the generation of successive particles. We constructed 14 sand piles poured from a point source, each containing about 6,500 particles. The individual simulations differ only by the initialization of the random number generator for the generation of particles. The particle corners are placed randomly on ellipses with uniformly distributed lengths of axes. For the simulations presented here, both lengths are drawn from independent distributions with a prescribed ratio of their averages. In the case of equiaxed particles (aspect ratio close to one), both extensions are chosen from the same distribution. Individual particle aspect ratios are then

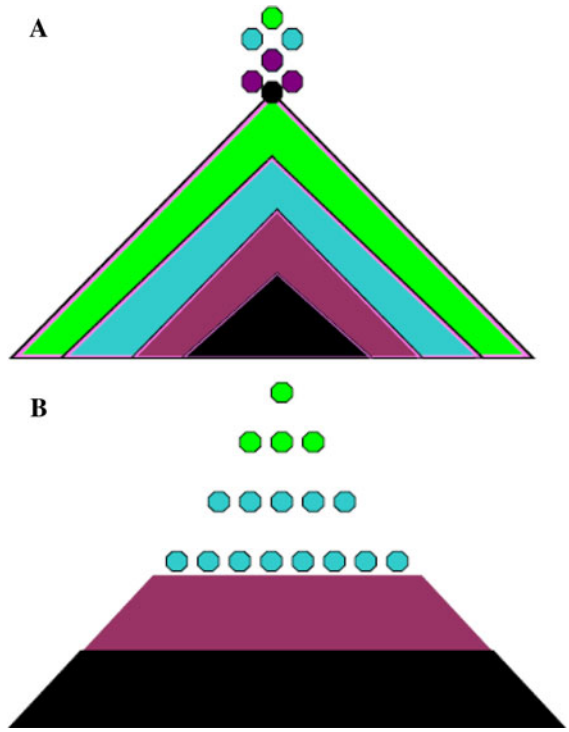

Fig. 1 Schematic diagrams of wedge sequence and layered sequence construction procedures of the sand pile. **a** Particles are dropped onto the apex of the pile, **b** Particles are dropped in a uniform distribution on each layer of the pile

limited by the width of this distribution (varying, for example, between 70% and 130% of the average). In the case of elongated particles to be discussed later, the second axis is drawn from a distribution, the average of which is by a certain factor smaller than that of the first, corresponding to the desired aspect ratio, and the polygon describing the particle was inscribed in an ellipse with the resulting (semi-)axes. Clearly, this procedure does not generate a fixed aspect ratio, the elongation of the particles and their shapes exhibit some variation—which is desired as it is just the same in nature—but the average aspect ratio takes a prescribed value (two for our elongated particles).

The 14 piles considered here consist of equiaxed particles, the number of polygon edges varies from six to eight for each simulation, and the average angle of repose for these piles was approximately 28°, obtained by taking the average over the left and right base angles.

In Sec 5, we will discuss the case of elongated particles with an average aspect ratio of 2. The number of particles and the degree of poly-dispersity were comparable in both systems. The average angle

of repose obtained for 10 piles was 31° for the mixture of elongated particles.

3.2 Sand Piles from a Line Source

Next, we constructed sand piles that consisted of about 6,500 convex equiaxed particles, pouring them from a line source. The dropping height of each new layer from the already present layer of the system was 8 mm (greater than one particle diameter) and particles were dropped uniformly onto the already present layer. The size and shape distribution of the particles were the same as that for the point source case. Also the time interval between two successive layers (not single particles) was 0.1 s. We constructed an ensemble of 11 sand piles using layered sequences. The measured average angle of repose of these sand piles was about 27°.

3.3 Simulation Parameters

We used a flat bottom ground plate onto which the material was poured. The characteristic properties of the ground plate, side walls and funnel (such as Young's modulus and friction coefficient) were equal to the particle properties. The average diameter of equiaxed particles was 6.8 mm, their degree of polydispersity was 30%. By this notion we describe a situation, where the minimum and maximum diameters are 6.8 mm plus minus 30% (i.e. the interval of possible axis lengths was [4.76 mm, 8.84 mm]), hence our degree of polydispersity refers to particle length scales, not their volume.

The static and dynamic friction coefficients of the particles were chosen equal for simplicity: $\mu_s = \mu_d = 0.54$. The density and Young's modulus of the particle were $\rho = 5{,}000\ kg/m^2$ and $Y = 10^7 N/m$, respectively. The time step for simulating the sand piles was $2 \times 10^{-6} s$ and the nondimensional coefficient of viscous damping described in (Roul et al. 2010; Schinner 2001) was $\gamma = 0.75$. This coefficient is used in the evaluation of a dissipative contribution $D_{\perp}^{*}$ to the force orthonormal to the contact line between two colliding particles, a force taken proportional to the velocity of change of the overlap area ΔA: $D_{\perp}^{*} = \gamma\sqrt{Ym_{\perp}}\Delta A/l\Delta t$, where $m_{\perp}$is an effective mass calculated from the properties of the two partners of the collision and l is the aforementioned characteristic length associated with the contact. For a detailed description of the defintions of $m_{\perp}$ and l as well as of the complete force calculation algorithm, the reader is referred to (Roul et al. 2010).

4 Calculation of Tensorial Fields

In this section, we give mathematical formulas for various macroscopic tensorial fields including stress, strain, and fabric for the sand piles. Note that the details on how the mathematical formulations for the macroscopic field quantities are derived from the microscopic ones and how averaging is performed to compute macroscopic variables are given in (Roul et al. 2010).

4.1 Calculation of Stress Fields

Once we have the forces and their points of contact, we can determine a formal stress tensor of a single particle, and then it is easy to determine the average of the stress tensor over many particles in a representative volume element (RVE). The stress tensor of a single particle can be expressed as follows:

$$\sigma_{ij} = \frac{1}{V^p}\sum_{c=1}^{n} r_i^c f_j^c, \tag{2}$$

where r_i^c is i-th component of the branch vector joining the centre of mass of the particle to the contact point c and f_j^c is the j-th component of the total force in that contact point. n is the number of contact points of the particle p. V^p is the volume of the particle (it is an area in two-dimensions).

This microscopic stress tensor would not be a convenient tool to describe the macroscopic pile, because it fluctuates wildly within a volume element containing just a few particles. In order to reduce fluctuations and to approach a macroscopic description, an RVE is defined by the requirement that the averaging procedure gives an unchanged result on increase of the volume element. In preceding numerical experiments (Roul et al. 2010), we have determined the necessary size of the RVE to correspond to 100-200 particles.

4.2 Calculation of Strain Fields

To determine strains, we first allow sand piles to relax under reduction of gravity. In this context, we change

gravity very slowly by about 10% from the ambient gravity level of the pile. The main reason for changing gravity is that this will lead to slight displacements of the particle centres, which allow us to obtain incremental strains by determining the position changes at the particle centres. As discussed in (Roul et al. 2010), the procedure can also be used to approximately determine the normal strain component aligned with the gravity vector by referring to a hypothetical strainless state at zero gravity, but fails for non incremental strain components along other directions.

We used a best-fit approach, proposed by Cambou and his coworkers (Cambou et al. 2000), who consider the relative translation of the particles. Assume that two particles p and q have a contact c and du_j^p and du_j^q denote the translations of the centres of particles p and q, respectively. Then the relative translation of two particles p and q forming contact c can be defined as follows:

$$d\Delta u_j^c = du_j^q - du_j^p. \tag{3}$$

According to Cambou et al., the best-fit translation gradient tensor ε_{ij} obtainable from these displacements is

$$\varepsilon_{ij} = \sum_k z_{ik} \sum_c d\Delta u_j^c l_k^c, \quad i,j,k = x,y, \tag{4}$$

where z_{ij} denotes the inverse of the matrix $\begin{pmatrix} \sum_{c=1}^{n} l_x^c l_x^c & \sum_{c=1}^{n} l_y^c l_x^c \\ \sum_{c=1}^{n} l_x^c l_y^c & \sum_{c=1}^{n} l_y^c l_y^c \end{pmatrix}$ for two-dimensional systems.

Here the vector l^c joins the centres of mass of the two particles having the common contact point c. If we call these particles p and q, we may define $l_i^c = r_i^{pc} - r_i^{qc}$, The quantities r_i^{pc} and r_i^{qc} are the (components of the) branch vectors connecting the corresponding particle centres to the contact point c.

The components of the averaged deformation gradient in two dimensions are as follows

$$\varepsilon_{xx}(x,y) = \sum_c d\Delta u_x^c \left(z_{xx} l_x^c + z_{xy} l_x^c\right)$$

$$\varepsilon_{yy}(x,y) = \sum_c d\Delta u_y^c \left(z_{yx} l_x^c + z_{yy} l_y^c\right)$$

$$\varepsilon_{yx}(x,y) = \sum_c d\Delta u_x^c \left(z_{yx} l_y^c + z_{yy} l_y^c\right)$$

The strain tensor u_{ij} is obtained from this by symmetrization, i.e. $u_{ij} = \frac{1}{2}\left(\varepsilon_{ij} + \varepsilon_{ji}\right)$.

4.3 Fabric Tensor

It is worth pointing out that the fabric tensor defines the internal texture of an assembly of particles. Once we have the contact points of the individual particles, we can calculate the fabric tensor for a single particle. The formula for the fabric tensor of particle p is given (Goddard 1998; Cowin 1988; Luding 2004; Lätzel et al. 2000) by

$$F_{ij}^p = \sum_{c=1}^{m} n_i^c n_j^c, \tag{5}$$

where n_i^c is the i-th component of the unit vector to contact point c of the considered particle p,

$$n_x^c = \frac{x_c - x_p}{\sqrt{(x_c - x_p)^2 + (y_c - y_p)^2}},$$

$$n_y^c = \frac{y_c - y_p}{\sqrt{(x_c - x_p)^2 + (y_c - y_p)^2}}, \tag{6}$$

where (x_c, y_c) and (x_p, y_p) are the contact point and the centre of mass of particle p, respectively. Hence, $\mathbf{n}^c$ is the direction of the branch vector to contact c. We take an average over sufficiently many particles in a representative volume element V to determine the average fabric tensor. The averaged fabric tensor can be written as

$$\langle F_{ij} \rangle_v = \frac{1}{V} \sum_p V^P F_{ij}^P, \tag{7}$$

where V is the volume of the averaging element that contains the particles whose centre of mass lies inside it and V^p and F_{ij}^p respectively denote the volume and the fabric tensor of particle p.

5 Simulation Results

In this section, first, we present the simulation results of the force network inside a sand pile, for two types of sand piles that were constructed using the two kinds of pouring protocols mentioned. Fig. 2a displays the force network for a point source sand pile. The line thickness represents the magnitude

(strength) of the force. The darker and wider a line the stronger the force it represents. In Fig. 2 b, we give the same results for a sand pile poured from a line source. As can be seen in the figure, the force network varies as a function of the position in the pile, exhibiting strong fluctuations. We observe that in the heap, there are weak force chains near the free surface of the pile and much stronger ones in the interior region near its middle, indicated as a thick horizontal (red/dark) line at the bottom of the picture. On the other hand, the force network for the pile poured from a point source demonstrates that there are no extremely strong force chains appearing in the central region of the pile.

Next, via averaging over representative volume elements (RVE), we have determined several macroscopic quantities, viz. stress, strain, fabric and density throughout the piles. We discuss in the following the simulation results of the averaged normalized (negative) stress tensor for the sand piles constructed by the two different pouring protocols. We normalized the stress tensor by the quantity ρgh, where ρ and h denote the average density and the height of the sand pile, respectively, and g is the acceleration due to gravity.

Since we find that fluctuations in the stress tensor field of a single sand pile are strong, we take averages over several piles in order to suppress these fluctuations somewhat. The vertical normal stress, averaged over 14 piles is displayed in Fig. 3 a, at different heights above the base of a point source pile consisting of a mixture of equiaxed particles. We find a pressure dip below the apex of the pile, which

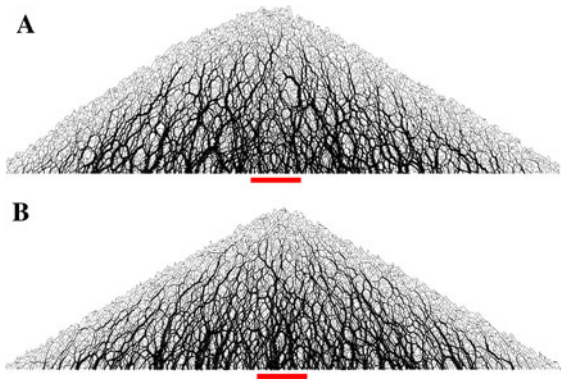

Fig. 2 Simulation result giving the force network for a sand pile constructed from a point source (**a**) and from a line source (**b**)

appears not only at the bottom, but also exists up to a certain height inside the piles. The vertical normal stress distribution inside a pile built from a line source, averaged over 11 piles, is shown in Fig. 3b. From the figure, we find there is no stress dip below the apex of the pile; it displays a plateau near the centre of the piles. Furthermore, we compare numerical simulation results of stress distributions with the results obtained by experimental measurement both for point source and line-source sand piles (Vanel et al. 1999).These comparisons exhibit identity of our numerical results and experimental ones in all qualitative respects. Of course, a quantitative comparison is not meaningful, because the experiments have been done for three-dimensional systems.

In the next step, we determine the vertical normal stress for sand piles constructed from a point source and consisting of a mixture of elongated particles, then compare the result with the stress tensor of sand piles containing equiaxed particles. Since our simulations are two-dimensional, we cannot simulate realistic particle shapes, but we try to mimic the difference between roughly spherical and elongated particles by working with almost circular (but polygonal) particles on the one hand and elongated ones inscribed into an ellipse on the other hand. As mentioned before, elongated particles with an average aspect ratio of 2 were used for the simulation.

Simulation results of the average negative vertical normal stress tensor for piles consisting of a mixture of elongated particles are illustrated in Fig. 4 a, which shows that the stress dip is clearly much larger below the apex of the pile than for the mixture of equiaxed particles, as represented in Fig. 3a. A quantitative comparison between the two sand piles at the bottom layer provides that the amplitude of the stress dip is about two times larger for the elongated particles than for equiaxed ones. The reason for the existence of the large dip in the centre of a sand pile consisting of elongated particles may be that the anisotropy of the contact network is larger in the central region than for the mixture of equiaxed particles. In conclusion, the stress tensor under a sand pile is affected by the shape distribution of particles.

In addition, the stress distributions inside piles consisting of equiaxed particles are compared with the stress tensor for a pile consisting of elongated particles, where particles are dropped using a line source. We have confirmed that the latter stress

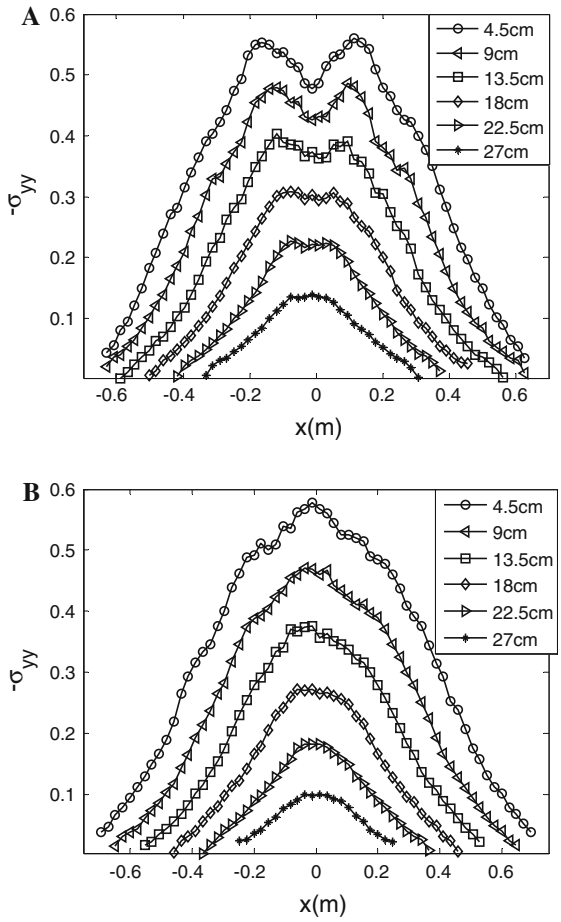

Fig. 3 Normalized vertical (negative) normal stress tensor component $-\sigma_{yy}$ at different heights inside the sand pile consisting of equiaxed particles, constructed from a point source (**a**) and from a line source (**b**)

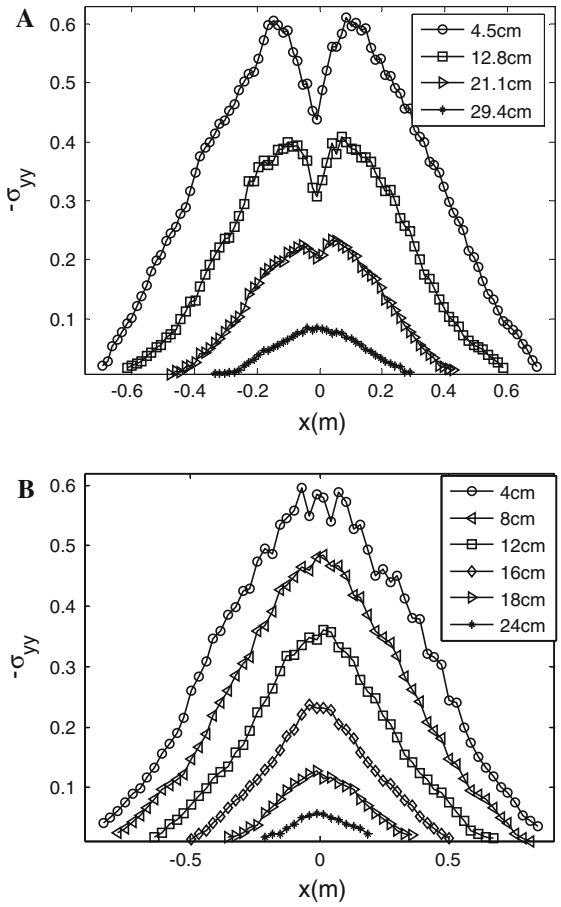

Fig. 4 Distribution of the vertical normal stress tensor $-\sigma_{yy}$ on horizontal cuts at different heights of the point source sand pile constructed from elongated particles. **a** Average over 10 sand piles poured from a point source. **b** Result for a single sand pile poured from a line source

distribution behaves qualitatively similar not showing a local minimum near the centre of the pile. Since this behaviour is expected and only mildly interesting, we have not done averages on several line-source piles, but we give an example of a single sand pile in Fig. 4 b.

We then compute the average volume fraction inside a sand pile constructed from a point source using equiaxed particles; this is illustrated in Fig. 5a, whereas the same quantity is represented in Fig. 5b for a line-source sand pile. For a point source, the central core region of the pile exhibits an increased density that is approximately 8-10% higher than the density in the vicinity of the surface of the pile. In contrast, the volume fraction is almost constant, close to 0.79, in the line source case, especially in the central region of the sand pile. Since in averaging the volume fraction over a representative volume element we discard particles whose centre of mass is not in the element, our values systematically underestimate the true volume fraction. (The procedure could be improved by including particles that are not completely in the representative volume element with a weight factor corresponding to their fraction inside it.) There is a slight inhomogeneity of the distribution in the vicinity of the surface of the sand pile. We conclude from our numerical investigation of the average density for the sand pile that the construction history of the granular aggregates affects their density distribution, which agrees with the existing experimental conclusion (Picard et al. 2001).

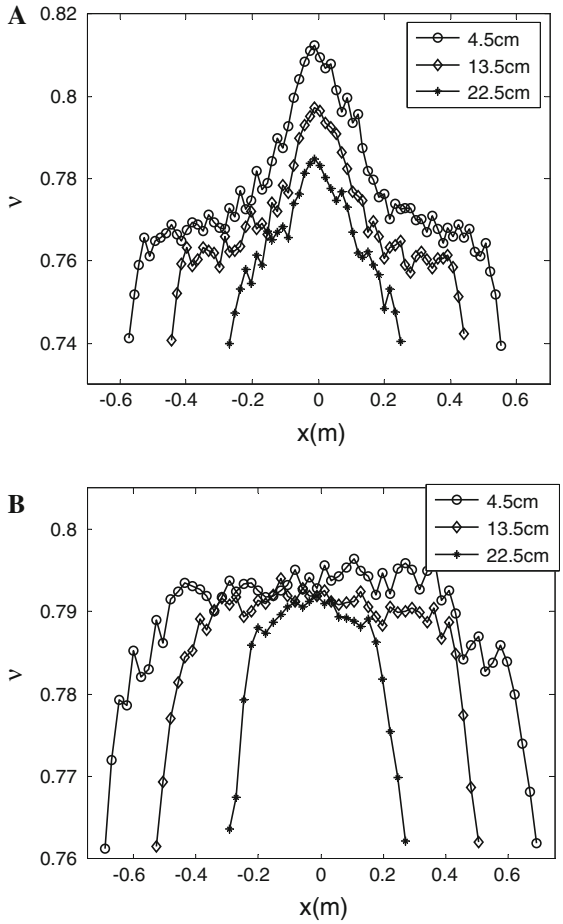

Fig. 5 Simulation results of the volume fraction v (which is proportional to the mass density) for sand piles created from a point source (**a**) and from a line source (**b**)

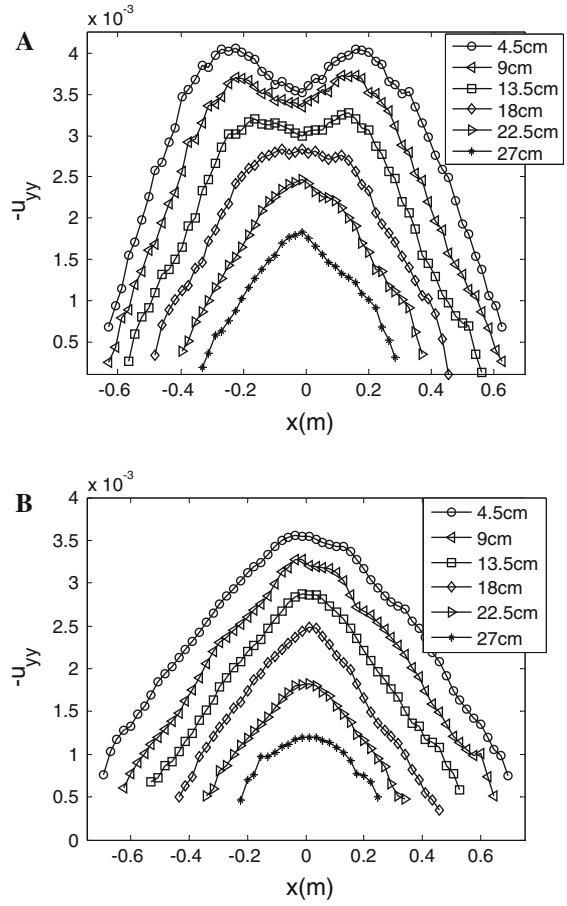

Fig. 6 Incremental vertical normal strain distribution $-u_{yy}$ obtained by a gravity reduction of 10%, at different heights of simulated sand piles, for sand piles poured from a point source (**a**) and from a line source (**b**). Note that the "true" strains with respect to a hypothetical zero gravity reference state would be larger by roughly a factor of 10

Our numerical measurements of the vertical incremental normal strains obtained by a change of gravity level by approximately 10% for two types of sand piles are displayed in Fig. 6. (An approximation to the full normal strain would be obtained by multiplying this with the appropriate factor, about 10. As discussed in (Roul et al. 2010), this procedure would not be exact, because lateral stresses were found not to scale with gravity and the vertical strain is also coupled to the horizontal stress. Quantitatively, the inaccuracy is limited for the vertical strain, whereas for horizontal ones the distinction between incremental strains that can be calculated accurately and nonincremtenal ones, which for lack of a reference state cannot, becomes important.) The figure reveals that the vertical normal strain changes with the layer position inside the piles like the stress tensor, as expected, which means the behaviour of this strain tensor component is qualitatively similar to that of the corresponding stress tensor component for a certain construction history of the pile. For a point source, we find a dip (Fig. 6 a) in the strain profile. A similar strain minimum was not obtained in sand piles constructed from a line source (Fig. 6 b).

The last ingredient missing for the macroscopic properties of a pile is the fabric tensor for describing the internal structure of the sand piles; in particular, we determine the contact density inside the piles. The trace of the averaged fabric at different heights for two types of sand piles is displayed in Fig. 7. For the case of a point source (Fig. 7 a), the isotropic part of the fabric has a maximum value exactly below the

apex of the piles, whereas for the case of a line source (Fig. 7 b), the fabric distribution in the middle of the pile remains flat and is almost constant, which means fabric is homogeneously distributed in the central region of the pile. This means that contact density and volume fraction are positively correlated, which is not too surprising.

In Fig. 8, we give the trace of the fabric tensor for a sand pile consisting of a mixture of elongated particles with average aspect ratio 2 poured from a point source, which exhibits a strong increase of the contact density near the centre of the pile with a peak that is even more pronounced than in the case of equiaxed particles (Fig. 7 a). It also underlines the close relationship between the existence of a minimum in the pressure and a maximum in the trace of the fabric, a somewhat counterintuitive correlation, as one would expect normally that a reduction of pressure also leads to a reduction of the contact density of particles.

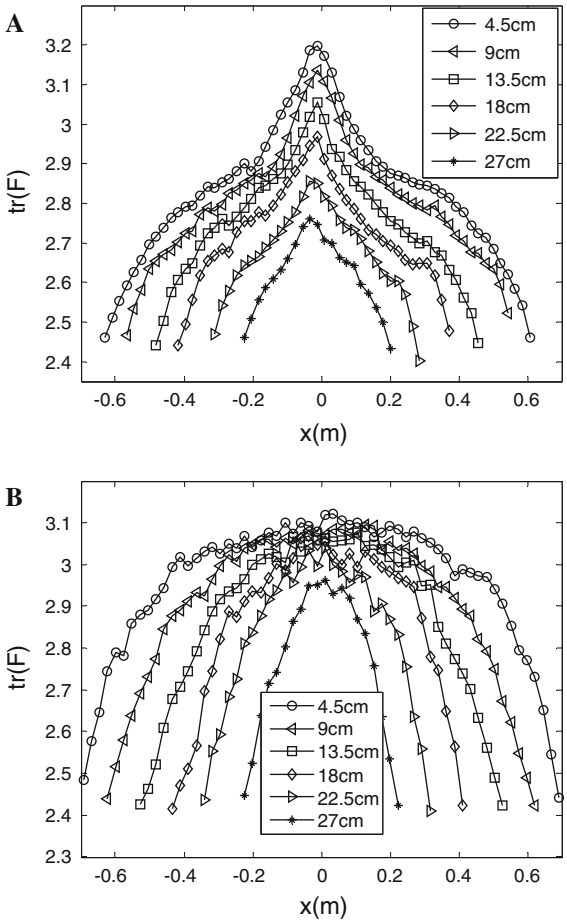

Fig. 7 Averaged trace of the fabric tensor F for sand piles consisting of equiaxed particles, created from a point source (**a**) and from a line source (**b**)

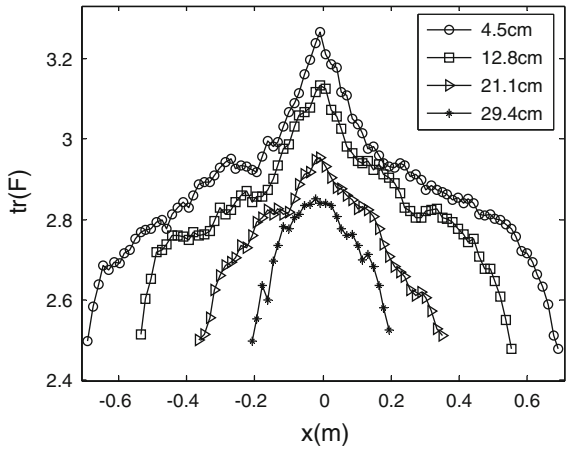

Fig. 8 The trace of the fabric tensor F for a point source sand pile consisting of a mixture of elongated particles

6 Stress Distribution of Asymmetric Sand Piles

In the next step, we simulate asymmetric sand piles using a point source procedure. A pile consists of roughly 5,900 equiaxed polygonal particles with average diameter of 9 mm and each particle having seven corners, the degree of poly-dispersity is 30%. The procedure for constructing an asymmetric pile from a point source is essentially the same as that of the construction of a symmetric sand pile, but instead of using a fixed-position point source (the funnel), we move the funnel horizontally towards the right-hand side. The average angle of repose for the left-hand side of the sand pile obtained for seven sand piles was 28° and it was 21° for the right-hand side of the sand pile. The funnel, originally positioned at $x = 0$, started moving after a certain temporal delay, so particles are falling on the inclined surface of an existing sand pile, once the funnel is in motion. From this consideration, it is relatively easy to understand why the left angle of repose was always larger than the right one.

Figure 9 shows an example of an asymmetric sand pile poured from a point source and one obtained using a line source. Different colours/grey levels correspond to groups of particles deposited at different times. The pile produced by layerwise deposition (Fig. 9 b) looks much more "tidy" than the one built

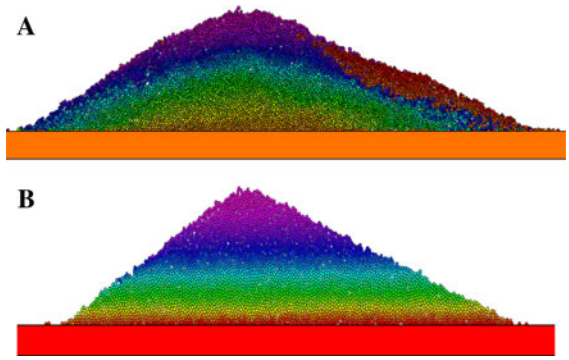

Fig. 9 Simulated asymmetric sand pile constructed from a point source (**a**) and from a line source (**b**). **a** Width of the pile at the bottom: 180 cm, height to the tip: 36 cm. **b** Width of the pile at the bottom: 110 cm, height to the tip: 23.5 cm

from a point source (Fig. 9 a) which has a roundish tip and non-straight surfaces, whereas the envelope of the line-source pile is almost a perfect triangle. The difference is due to the continuous generation of avalanches in the process of pouring the point source pile; these produce disorder in the surface profile, whereas avalanches are essentially absent in the case of a pile growing from a line source with deposition at small kinetic energy.

We present in Fig. 10a the numerical results of the averaged (negative) vertical normal stress tensor at different heights of an asymmetric pile constructed from a point source. The topmost curve in the graph shows the stress tensor result at the bottom layer of the corresponding sand pile, whereas the bottom curve corresponds to the top layer. It can be seen that there is an asymmetric stress distribution and a dip exists in the stress profile below the apex of the sand piles. Also, due to the movement of the point source to the right, the minima of the pressure distribution at different heights are shifted from $x = 0$ to values between $x = 0.1$ and $x = 0.2$ in the course of time. The precise value of the final shift depends on the lateral velocity of the source as well as on the duration of the procedure and no attempt was made to control it in the simulation.

Furthermore, we obtain an asymmetric sand pile by constructing it from about 3,700 polygonal particles that are poured from a line source. Particles used were equiaxed with a fixed number of corners (seven) for individual simulations, an average diameter of 7 mm, and the degree of polydispersity was 10%. The procedure for constructing an asymmetric

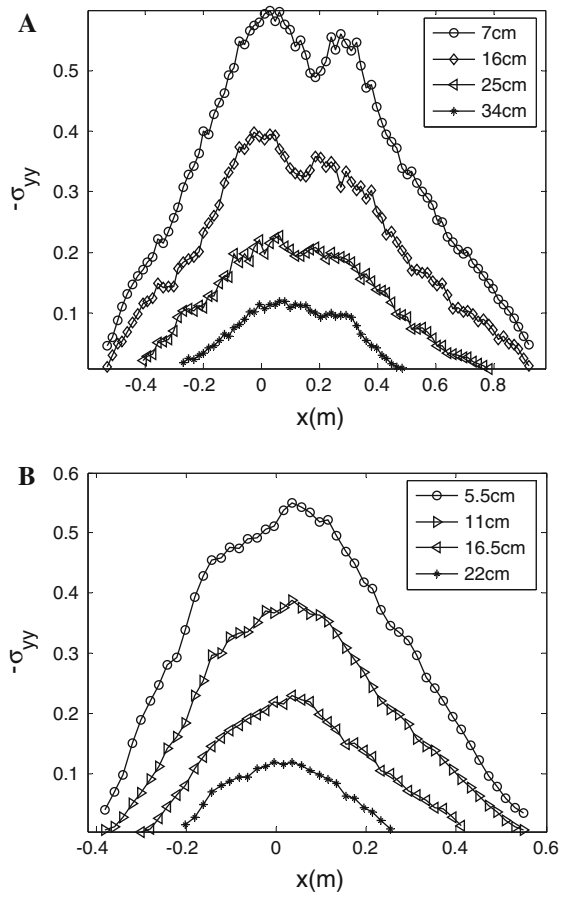

Fig. 10 Simulation result for the vertical normal stress distribution $-\sigma_{yy}$(normalized) at various heights inside a two-dimensional asymmetric sand pile constructed from a point source (**a**) and a line source (**b**)

sand pile from a line source is based on a similar line of thought as the construction of the symmetric sand pile, but instead of depositing a new layer onto an already present one symmetrically we deposit it in an asymmetric way, shifting the centre of the line source in each deposition step by a constant amount to the right (again after some initial delay during which a small pile was allowed to build up). The average angle of repose obtained for seven sand piles was 31° for the left-hand side of the pile and 22° for the right-hand side of the pile.

Figure 10 B shows the simulation results for the averaged normalized (negative) vertical normal stress tensor along horizontal cuts at different heights of an asymmetric sand pile constructed from a line source. From the figure, we find an asymmetric pressure distribution under an asymmetric sand pile, as

expected and a plateau distribution below the apex of the pile. No experimental results seems to exist in the literature to which we might compare our numerical simulation results. However, qualitatively similar behaviour was observed in the analytical approach for sand piles obtained by Didwania et al. (Didwania et al. 2000) who calculated the asymmetric stress distribution below the apex of the asymmetric sand pile in the framework of an elastoplastic model.

Our results on the stress distribution in an asymmetric pile make for an interesting corollary on ideas discussed in (Wittmer et al. 1997), concerning the "freezing in" of a stress distribution or at least its orientational characteristic as soon as a grain is buried in the deposition process. This is a basic assumption motivating the fixed-principal axis model (FPA) proposed in (Wittmer et al. 1997). Looking closely at the curves in Fig. 10 a, we note that by and large the extrema appear to move from the right to the left when we go from a lower layer of the sand pile to an upper one. (Remember that earlier layers are at the bottom of the pile, later ones at the top.) If stress distributions in a layer were frozen as soon as it was buried by the next layer of grains, we would expect motion from left to right, which is the direction of motion of the point or line source. That this does not happen demonstrates clearly that the stress distribution is changing *throughout the pile* as new layers are added, reducing the credibility of the FPA assumption.

In Fig. 11, we give the trace of the fabric tensor for asymmetric sand piles built both from a point source and from a line source. Both distributions display a certain degree of asymmetry beyond the displacement of their centre to the right and show that also the contact distribution has some flexibility in adapting to the deposition of later layers of particles. Therefore, while these quantities are history dependent, they are not immutable by later events and a change in the construction protocol will modify the observed distribution in situ.

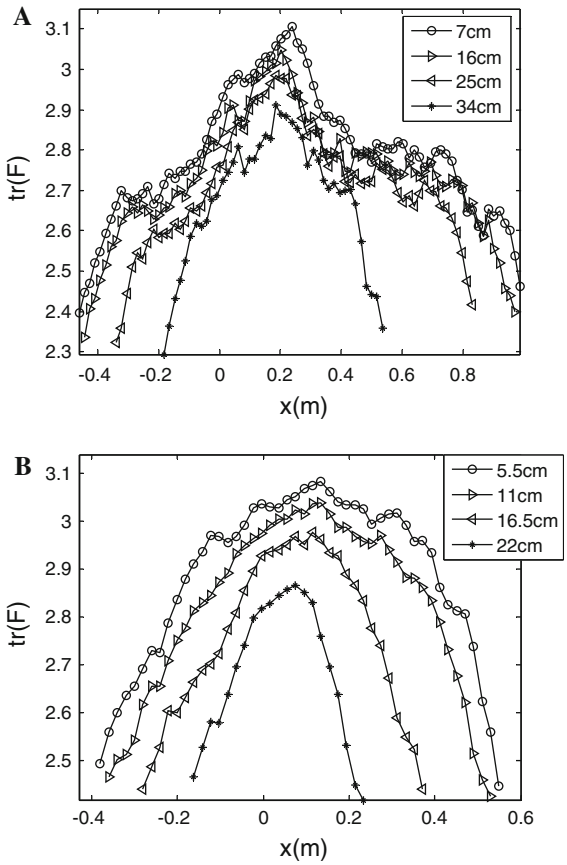

Fig. 11 The trace of the fabric tensor F for an asymmetric sand pile built from a point source (**a**) and a line source (**b**)

7 Conclusions

To conclude, numerical simulations were performed on two-dimensional systems, in which a symmetric sand pile was constructed from several thousands of convex polygonal particles with varying shapes, sizes and edge numbers. The particles were poured either from a point source or a line source. We measured microscopic force distributions of the resulting sand piles. We find that force networks exist and strongly fluctuate within the sand pile and that the building history of the heap influences the structure of the force chains.

Determining numerically the stress fields inside the pile, the averaged stress distribution reproduces the experimentally observed pressure minimum for sand piles poured from a point source, whereas a similar minimum was not observed for sand piles built from a line source. This confirms that two sand piles consisting of the same material may have different stress distributions.

Moreover, the averaged stress tensors were compared numerically for sand piles consisting of equiaxed particles with those from sand piles consisting of elongated particles. We obtained a small dip below the apex of piles that contain a mixture of equiaxed particles when the pile was constructed by dropping

particles from a point source, whereas the stress dip is clearly much larger for the case of elongated particles. Comparing the magnitude of the stress dip at the bottom layer of the piles, we note that the amplitude of the stress dip is two times larger for the elongated particles of average aspect ratio two. Therefore, not only the construction history of the sand pile affects the pressure distribution under a sand pile, but also the shape of the particles.

The averaged density was obtained for both types of sand piles. We found that the central core region of the point source heap displays a higher density than its surroundings, which is a surprising finding, because the density increases where the pressure becomes smaller. A detailed discussion of the physical implications of such a behaviour is given in (Roul et al. 2010). On the other hand, we did not find much deviation in the density profile for a line-source heap; the volume fraction is approximately homogeneously distributed in the central region of the pile.

The averaged vertical normal strain tensor was evaluated numerically throughout the sand pile, for two types of sand piles. The outcome of the simulation for a point source pile, which resembles the vertical normal stress, gives a minimum not only at the bottom layer but also in higher layers of the sand piles, as expected. Again, the situation is different for a pile poured from a line source, which demonstrates that the construction history affects the strain distribution under a sand pile.

Another macroscopic tensorial quantity that we determined was the fabric tensor in order to gain more detailed knowledge on overall macroscopic material properties of the sand piles. An interesting observation has been made in our numerics: in the *lower* pressure region in the centre of the sand piles created by the point source protocol, we have a *higher* number of average contacts of the particles. While this behaviour of the contact density is counterintuitive in terms of the pressure, it fits together well with the increased local density in the centre. Moreover, the contact number density is affected by the filling method of the granular aggregates.

Finally, the averaged stress distributions were measured numerically inside asymmetric sand piles as well that were constructed using two different pouring protocols. We emphasize that the stress fields inside an asymmetric sand pile have not been previously measured experimentally. Measuring the stress distribution under the sand piles we found that the construction history of the granular aggregates affects their stress distributions.

Acknowledgments We are grateful to Prof. S. Luding for valuable suggestions and fruitful discussions on the computational results illustrated in this work. We would like to acknowledge the Deutsche Forschungsgemeinschaft (DFG) for financial support of this project within the graduate school 828.

References

Azéma E, Radjai F (2010) Stress-strain behavior and geometrical properties of packings of elongated particles. Phys Rev E 81:051304

Bouchaud J-P, Cates ME, Claudin P (1995) Stress distribution in granular media and nonlinear wave equation. J Phys I France 5:639–656

Brockbank R, Huntely JM, Ball R (1997) Contact force distribution beneath a three dimension-al granular pile. J Phys II France 7:1521–1532

Cambou B, Chaze M, Dedecker F (2000) Change of scale in granular materials. Eur J Mech A Solids 19:999–1014

Cantelaube F, Goddard JD (1997) Elastoplastic arching in 2D granular heaps. In: Behringer RP, Jenkins JT (eds) Powders and Grains. Balkema, Rotterdam, pp 231–234

Claudin P, Bouchaud J-P, Cates ME, Wittmer J (1998) Models of stress fluctuations in granular media. Phys Rev E 57:4441

Cowin SC (1988) A simple theory of instantaneously induced anisotropy. In: Jenkins JT, Satake M (eds) Micromechanics of granular materials. Elsevier, Amsterdam, pp 71–80

Cundall PA, Strack ODL (1979) A discrete numerical model for granular assemblies. Géote-chnique 29:47–65

Didwania AK, Cantelaube F, Goddard JD (2000) Static multiplicity of stress states in granular heaps. Proc R Soc Lond A 456:2569–2588

Gear CW (1971) Numerical initial value problems in ordinary differential equations. Prentice Hall, Englewood Cliffs, NJ

Goddard JD (1998) Continuum modeling of granular assemblies. In: Herrmann HJ, Hovi JP, Luding S (eds) Physics of dry granular media. Kluwer Academic Publishers, Dordrecht, pp 1–24

Hidalgo RC, Zuriguel I, Maza D, Pagonabarraga I (2009) Role of particle shape on the stress propagation in granular packings. Phys Rev Lett 103:118001

Jotaki T, Moriyama R (1979) On the bottom pressure distribution of the bulk materials piled with the angle of repose. J Soc Powder Technol 16(4):184–191

Lätzel M, Luding S, Herrmann HJ (2000) Macroscopic material properties from quasi-static, microscopic simulations of a two-dimensional shear-cell. Granular Matter 2:123–135

Li YJ, Xu Y, Thornton C (2005) A comparison of discrete element simulations and experiments for 'sand piles' composed of spherical particles. Powder Technol 160: 219–228

Liffman K, Nguyen M, Metcalfe G, Cleary P (2001) Forces in piles of granular material: an analytic and 3D DEM study. Granular Matter 3:165–176

Luding S (2004) Micro-macro models for anisotropic granular media. In: Vermeer PA, Ehlers W, Herrmann HJ, Ramm R (eds) Modelling of cohesive-frictional materials. Balkema AA, Leiden, pp 195–206

Luding S (1997) Stress distribution in static two-dimensional granular model media in the absence of friction. Phys Rev E 55:4720–4729

Matuttis HG (1998) Simulation of the pressure distribution under a two dimensional heap of polygonal particles. Granular Matter 1:83–91

Matuttis HG, Luding S, Herrmann HJ (2000) Discrete element simulations of dense packings and heaps made of spherical and non-spherical particles. Powder Technol 109:208–292

Picard D, Terzulli LP, Lesaffre C, Mineau V (2001) Packing density of a poly-dispersed granular material. In: Kishino Y (ed) Powders and grains. Balkema, Rotterdam, pp 15–16

Roul P, Schinner A, Kassner K (2010) Mechanical properties of non-cohesive polygonal particle aggregates, Granular Matter (online first). doi: 10.1007/s10035-010-0228-1

Schinner A (1999) Fast algorithms for the simulation of polygonal particles. Granular Matter 2:35

Schinner A (2001) Ein simulationssystem für granulare aufschüttungen aus teilchen variabler form. PhD thesis, University of Magdeburg

Smid J, Novosad J (1981) Pressure distribution under heaped bulk solids. Proc Powtech Conf Ind Chem Eng Sympo Series 63: D3/V/1–12

Smid J, Xuan PV, Thyn J (1993) Effect of filling method on the packing distribution of a catalyst bed. Chem Eng Technol 16:114–118

Tejchman J, Wu Wei (2008) FE-Calculations of stress distribution under prismatic and conical sand piles within hypoplasticity. Granular Matter 10:399–405

Vanel L, Howell D, Clark D, Behringer RP, Clement E (1999) Memories in sand: experimental tests of construction history on stress distributions under sand piles. Phys Rev E 60:R5040

Wittmer JP, Cates ME, Claudin P, Bouchaud J-P (1996) An explanation for the stress minimum in sand piles. Nature 382:336–338

Wittmer JP, Cates ME, Claudin P (1997) Stress propagation and arching in static sand piles. J Phys I France 7:39–80

Zhao YC, Xu BH, Zou RP, Yu AB, Zulli P (2003) Stress distribution in a sand pile formed on a deflected base. Adv Powder Technol 14:401–410

Zuriguel I, Mullin T, Rotter JM (2007) Effect of particle shape on the stress dip under a sand pile. Phys Rev Lett 98: 028001

Zuriguel I, Mullin T (2008) The role of particle shape on the stress distribution in a sand pile. Proc R Soc A 464: 99–116